

# Structural and functional properties of spatially embedded scale-free networks

Thorsten Emmerich,<sup>1</sup> Armin Bunde,<sup>1</sup> and Shlomo Havlin<sup>2</sup>

<sup>1</sup>*Institut für Theoretische Physik, Justus-Liebig-Universität Giessen, 35392 Giessen, Germany*

<sup>2</sup>*Department of Physics, Bar-Ilan University, Ramat-Gan 52900, Israel*

(Received 16 January 2014; published 10 June 2014)

Scale-free networks have been studied mostly as non-spatially embedded systems. However, in many realistic cases, they are spatially embedded and these constraints should be considered. Here, we study the structural and functional properties of a model of scale-free (SF) spatially embedded networks. In our model, both the degree and the length of links follow power law distributions as found in many real networks. We show that not all SF networks can be embedded in space and that the largest degree of a node in the network is usually smaller than in nonembedded SF networks. Moreover, the spatial constraints (each node has only few neighboring nodes) introduce degree-degree anticorrelations (disassortativity) since two high degree nodes cannot stay close in space. We also find significant effects of space embedding on the hopping distances (chemical distance) and the vulnerability of the networks.

DOI: [10.1103/PhysRevE.89.062806](https://doi.org/10.1103/PhysRevE.89.062806)

PACS number(s): 64.60.aq, 89.75.-k, 05.10.Ln

## I. INTRODUCTION

Many complex systems can be well represented as networks, which helps to understand their structural and functional properties. These complex systems can be man-made structures such as the World Wide Web, transportation systems, and power grid networks or natural systems such as proteins or the network of neurons in the brain [1–3].

When studying the properties of such networks it is usually assumed that spatial constraints can be neglected. However, in many cases where the Euclidean distance matters, this assumption may not be justified. Typical examples of those systems include the Internet, airline networks, wireless communication networks, and social networks that all are embedded on the surface of Earth, i.e., in two-dimensional space. Other examples include proteins and the neuronal web in the brain which both are embedded in three dimensions.

Two basic models of networks have been extensively studied: Erdős-Rényi (ER) graphs [4–6] and Barabasi-Albert scale-free (SF) networks [7–9]. While in ER networks the distribution of the number  $k$  of links per node (degree distribution) is Poissonian, in SF networks the distribution follows a power law  $P(k) \sim k^{-\alpha}$ , where  $\alpha$  is typically between 2 and 3.

In previous studies [10–13], we focused on ER-type networks embedded in one- and two-dimensional lattices of length  $L$  (for earlier studies in the same direction but with less conclusive results, see [14–16]). We assumed that the nodes are connected to each other with a probability  $p(r) \sim r^{-\delta}$ , where  $r$  is the Euclidean distance between the nodes. This choice of  $p(r)$  is supported by findings in the Internet, airline networks, human travel networks, and other social networks [17–19]. Our results suggested that the exponent  $\delta$  controls the dimension  $d$  of the embedded network, which continuously varies between  $d = \infty$  for  $\delta < d_e$  and  $d = d_e$  for  $\delta$  above  $2d_e$ , where  $d_e$  is the embedding dimension of the underlying lattice [13,20]. The mean topological distance (mean shortest path between all pairs of nodes in the network) scales with the network size  $N$  as  $\langle \ell \rangle \sim (\ln N)^\gamma$  for  $\delta$  below  $2d_e$ , with  $\gamma$  monotonously increasing,  $\gamma = 1$  for  $\delta < d_e$  to  $\gamma \rightarrow \infty$

at  $\delta = 2d_e$ . For  $\delta$  above  $2d_e$ ,  $\langle \ell \rangle$  increases by a power law. The percolation properties are not drastically changed by the spatial constraints: The percolation threshold increases with  $\delta$  [11].

Here we focus on SF-type networks embedded in two-dimensional lattices ( $d_e = 2$ ) with the same link-length distribution  $p(r) \sim r^{-\delta}$ . Our model of embedding links of length  $r$  in a two-dimensional lattice can be regarded as a generalization of the two known models, the Watts-Strogatz model [21,22] and the Kleinberg model [23]. In both models, long-range links are added in a lattice system. In the Watts-Strogatz model all link lengths are chosen with the same probability, while in the Kleinberg model the link lengths are chosen from a power law distribution  $p(r) \sim r^{-\delta}$  as in the case considered here. Other methods for embedding networks in Euclidean space have been proposed in [24–29].

We are interested in studying how in SF-type networks characterized by the degree exponent  $\alpha$  the spatial constraints quantified by the distance exponent  $\delta$  modify the structural and functional properties of the networks. Examples of embedded SF networks are the Internet, airline networks, and social networks like friendship and author networks. Due to the hubs in the SF networks, their embedding in space is more elaborate than the embedding of ER networks and requires a dilution of the underlying lattice.

The article is organized as follows. In Sec. II, we briefly discuss the characteristic distances in the spatially constrained networks. Then, in Sec. III we describe in detail how the spatially embedded SF networks can be generated. In the following Results section (Sec. IV) we discuss how the degree exponent  $\alpha$  and the spatial exponent  $\delta$  (i) determine the properties of the maximum degree  $k_{\max}$  in the network and its scaling with the network size  $N$  and (ii) lead to degree-degree anticorrelations that increase with increasing  $\delta$  and decreasing  $\alpha$ . We also show (iii) how the scaling of the mean topological distance  $\langle \ell \rangle$  is modified by the spatial constraints and study (iv) how the vulnerability of the network depends on both  $\alpha$  and  $\delta$ . In addition, we discuss the dimension of the embedded SF networks and show that it is infinity for all  $\delta$  below  $2d_e$  and  $\alpha$  between 2 and 3.

## II. CHARACTERISTIC DISTANCES

First we estimate how the characteristic distances in the network (embedded in a square lattice) depend on its linear size  $L$  and on the spatial exponent  $\delta$ . The normalized distance distribution  $p(r)$  is

$$p(r) = \begin{cases} (d_e - \delta)L^{-(d_e - \delta)} r^{-\delta}, & \delta < d_e, \\ (\delta - 2d_e) r^{-\delta}, & \delta > d_e. \end{cases} \quad (1)$$

From  $p(r)$  we obtain the moments  $\bar{r}^n = \int_1^L dr r^{d_e - 1} r^n p(r)$  and the related length scales  $\bar{r}_n \equiv (\bar{r}^n)^{1/n}$ . The maximum distance  $r_{\max}$  is determined by  $L^{d_e} \int_{r_{\max}}^L dr r^{d_e - 1} p(r) \simeq 1$ . The results for  $\bar{r}^n$  and  $r_{\max}$  are

$$\bar{r}^n = \begin{cases} \frac{d_e - \delta}{d_e + n - \delta} L^n, & \delta < d_e, \\ L^n / \ln(L), & \delta = d_e, \\ \frac{\delta - d_e}{d_e + n - \delta} L^{d_e + n - \delta}, & d_e < \delta < d_e + n, \\ n \ln(L), & \delta = d_e + n, \\ \frac{d_e - \delta}{d_e + n - \delta}, & \delta > d_e + n, \end{cases} \quad (2)$$

and

$$r_{\max} \simeq \begin{cases} L, & \delta < 2d_e, \\ L^{d_e / (\delta - d_e)}, & \delta \geq 2d_e. \end{cases} \quad (3)$$

Accordingly, for  $\delta < d_e$  all length scales ( $\bar{r}_n$  and  $r_{\max}$ ) are proportional to  $L$ , the spatial constraints are irrelevant and the system can be regarded as an infinite-dimensional system. On the other hand, for  $\delta > 2d_e$ ,  $\bar{r}_n/L$  and  $r_{\max}/L$  tend to zero in the asymptotic limit. In this case, we expect that the physical properties of the network are close to those of regular lattices of dimension  $d_e$ . However, large finite size effects are expected for  $\delta$  close to  $2d_e$ , where  $r_{\max}/L$  decays only very slowly to zero. In the intermediate  $\delta$  regime  $d_e \leq \delta < 2d_e$ ,  $r_{\max}$  scales as  $L$ , while  $\bar{r}_n/L$  tends to zero in the asymptotic limit. Here we study how in this intermediate regime the topological and functional properties of the SF networks depend on the spatial constraints quantified by the spatial exponent  $\delta$ . We focus on networks embedded in a square lattice where  $d_e = 2$ .

## III. ALGORITHM FOR GENERATING EMBEDDED SCALE-FREE NETWORKS

Our aim is to generate embedded SF networks in two-dimensional space. The method is quite general and can be easily modified to generate any kind of degree distribution in any dimension. For simplicity, we consider networks that are embedded in a square lattice of size  $L \times L$ . The nodes of the network are the lattice sites and the links between them will be determined by the algorithm. To each node  $i$ , we assign  $k_i$  links from the distribution  $P(k) \sim k^{-\alpha^*}$ , with the minimum degree  $k_{\min} = 3$ . The lengths of the links are taken from the power law distribution (1). The algorithm consists of the following steps.

(1) We choose randomly a node  $i$  with a probability that is proportional to its available (unoccupied) links. To realize this, we choose randomly one of the available links in the network.

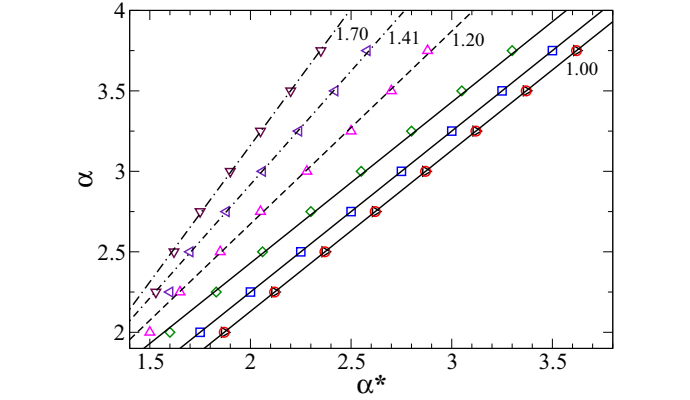


FIG. 1. (Color online) The degree exponent  $\alpha$  as function of the input exponent  $\alpha^*$  of SF networks for the spatial exponents  $\delta = 0$  ( $\circ$ ), 1.0 ( $\square$ ), 2.0 ( $\diamond$ ), 2.5 ( $\triangle$ ), 3.0 ( $\triangleleft$ ), 3.5 ( $\blacktriangle$ ), and 4.0 ( $\nabla$ ). The straight lines are best fits to the data with the slopes indicated in the figure. For each parameter set we averaged over 50 configurations.

(2) We choose randomly a distance  $r$  from  $p(r)$ , Eq. (1), and consider all nodes that are at a distance between  $r$  and  $r - \Delta$  from node  $i$ .

(3) We specify the available (unoccupied) links between node  $i$  and the other nodes in this annulus.

(4a) If there are available links, we choose one of them randomly and identify the node  $j$  this link belongs to. If nodes  $i$  and  $j$  are unconnected, we connect them by an edge and go back to step (1).

(4b) Otherwise, we keep the distance  $r$  chosen in (2), but choose randomly, as described in step (1), another node  $i$  as center of the annulus and continue with step (3). We repeat this process, with fixed  $r$ , up to 5 times, and then go back to step (1).

(5) We stop the process when the number of occupied edges exceeds  $L \times L$ . This way, we generate diluted SF networks. If we add more links to the network, both relevant power laws describing link-length and degree distributions cannot be simultaneously fulfilled. In the diluted networks, the number of nodes  $N$  is proportional to  $L^2$ ,  $N = cL^2$ , with  $c \simeq 0.45, 0.6, 0.7$ , and  $0.77$  for  $\alpha = 2, 2.5, 3$ , and  $3.5$ , respectively. Accordingly, the average degree of a node is  $2/c$  and thus varies between 2.6 (for  $\alpha = 4$ ) and 4.5 (for  $\alpha = 2$ ). These values compare with the values of real-world spatially embedded SF networks, for example, power grids, where the average degree ranges between 2.5 and 3 [30].

We consider square lattices up to a length of  $L = 1600$ . We find that due to the spatial constraints, in particular for large values of  $\delta$ , large embedded SF networks with small input parameter  $\alpha^*$  could not be generated.

The scaling exponent  $\alpha$  of the generated networks is always larger than the input exponent  $\alpha^*$  (see Fig. 1). This is since many outgoing links from high degree nodes cannot find nearby available nodes. Figure 1 shows how the output  $\alpha$  depends on the input  $\alpha^*$  for different values of  $\delta$ . The figure suggests that  $\alpha$  increases linearly with  $\alpha^*$ . The proportionality constant is 1 for  $\delta = 0, 1, 2, 2.5$  and increases with increasing  $\delta$ . Note that even for  $\delta = 0$ ,  $\alpha$  is slightly larger than  $\alpha^*$ , which we can attribute to the constraints of the finite lattice we

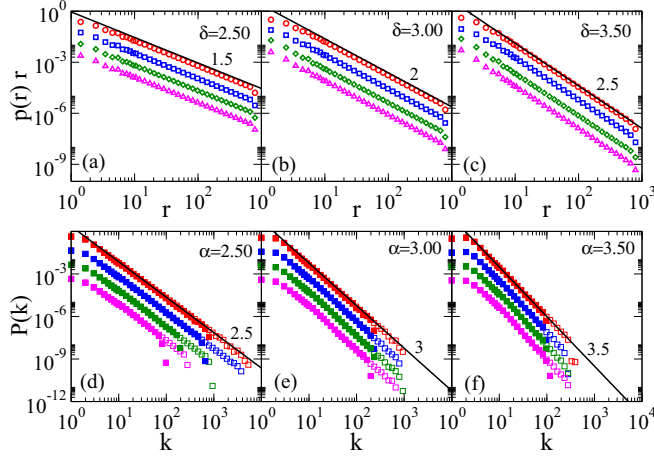


FIG. 2. (Color online) Link length distribution and degree distribution in spatially embedded SF networks. (a)–(c) The probability density  $p(r)r$  as function of the Euclidean link length of SF networks embedded in an  $800 \times 800$  lattice for the spatial exponents  $\delta = 2.5, 3.0$ , and  $3.5$  and the degree exponents  $\alpha = 2.25$  ( $\circ$ ),  $2.50$  ( $\square$ ),  $3.00$  ( $\diamond$ ),  $3.50$  ( $\triangle$ ) (from top to bottom). (d)–(f) Degree distribution  $P(k)$  as function of  $k$  for SF networks embedded in  $800 \times 800$  and  $400 \times 400$  lattices with degree exponents  $\alpha = 2.50, 3.00$ , and  $3.50$  [from panel (d) to panel (f)]. The spatial exponents are (from top to bottom)  $\delta = 1.0$  ( $\circ$ ),  $2.5$  ( $\square$ ),  $3.0$  ( $\diamond$ ),  $3.5$  ( $\triangle$ ). For the smaller lattice, the symbols are solid. For transparency, the lower plots in each panel have been shifted vertically (down) by factors of 10. The straight lines are guidelines with the expected slopes  $\delta - 1$  in (a)–(c) and  $\alpha$  in (d)–(f). For each parameter set we averaged over 50 configurations.

consider here. The figure also shows that for  $\alpha = 2$ , due to the competition between hubs and spatial constraints, networks with  $\delta$  above 3 could not be generated. Thus, in the following, we focus on  $\alpha \geq 2.25$ .

Figures 2 shows, as a quality test of the generated networks, the distributions of the link length  $r$  [panels (a), (b), (c)] and the degree  $k$  [panels (d), (e), (f)]. In the double logarithmic plots, the distributions nicely follow straight lines with slopes  $\delta$  and  $\alpha$ , respectively, confirming numerically that the generated networks with  $\alpha \geq 2.25$  are SF with the anticipated power law link length distribution.

## IV. RESULTS

### A. Maximum degree $k_{\max}$

In nonembedded SF networks, the maximum degree in a network consisting of  $N$  nodes scales as [31]  $k_{\max} \sim N^{1/(\alpha-1)}$ . Here we are interested to test how this relation is affected by the spatial constraints. To evaluate  $k_{\max}$ , we determined the maximum degrees in 50 networks and averaged them logarithmically. Figure 3 shows that  $k_{\max}$  scales with  $N$  by a power law,

$$k_{\max} \sim N^{1/(\alpha_{\text{eff}}-1)}, \quad (4)$$

where  $\alpha_{\text{eff}}$  depends on both the scaling exponent  $\alpha$  and the spatial exponent  $\delta$ . In random SF networks without spatial constraints,  $\alpha_{\text{eff}} = \alpha$  [31]. Figure 4 suggests that there exists a critical value of  $\delta$ . For  $\delta$  below this critical value, we have  $\alpha_{\text{eff}} = \alpha$ . For  $\delta$  above this critical value,  $\alpha_{\text{eff}}/\alpha$  seems to

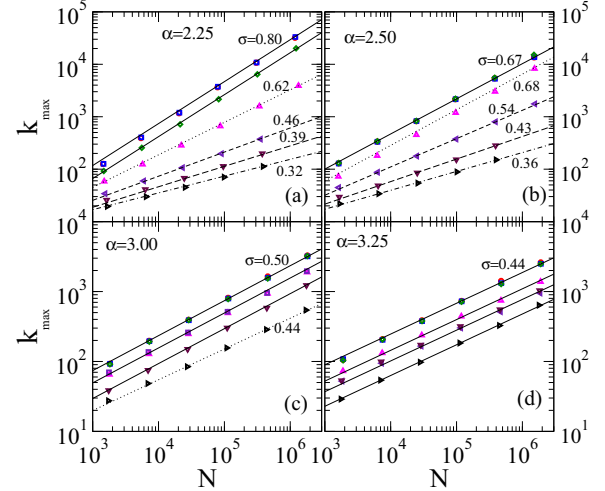


FIG. 3. (Color online) The cutoff  $k_{\max}$  as function of the size  $N$  of the generated SF networks with degree exponents  $\alpha = 2.25, 2.50, 3.00$  and  $3.25$  [from panel (a) to panel (d)] and the spatial exponents (from up to down)  $\delta = 0$  ( $\circ$ ),  $1.0$  ( $\square$ ),  $2.0$  ( $\diamond$ ),  $2.5$  ( $\triangle$ ),  $3.0$  ( $\triangleleft$ ),  $3.5$  ( $\nabla$ ), and  $4.0$  ( $\triangleright$ ). The straight lines are best fits to the data with slope  $\sigma$ . For transparency some curves have been shifted (up) on the  $y$  axis by the following factors  $f$ : panel (b) for  $\delta = 0, 1.0, 2.0$  by  $f = 1.5$ ; panel (c) for  $\delta = 0, 1.0, 2.0$  by  $f = 1.5^2$  and  $\delta = 2.5, 3.0$  by  $f = 1.5$ ; panel (d) for  $\delta = 0, 1.0, 2.0$  by  $f = 1.5^3$  and  $\delta = 2.5, 3.0$  by  $f = 1.5^2$ , and  $\delta = 3.5$  by  $f = 1.5$ .

increase linearly with  $\delta$ . This effect can be understood as follows. With increasing  $\delta$ , the mean link length decreases and thus only smaller hubs can be accommodated. For larger  $\alpha$  values, one needs to accommodate on the lattice only comparatively small hubs. In this case, the spatial constraint is weaker and thus the critical  $\delta$  value increases.

### B. Anticorrelations

Next we evaluate the degree-degree correlations in the spatially embedded networks and how they depend on  $\delta$

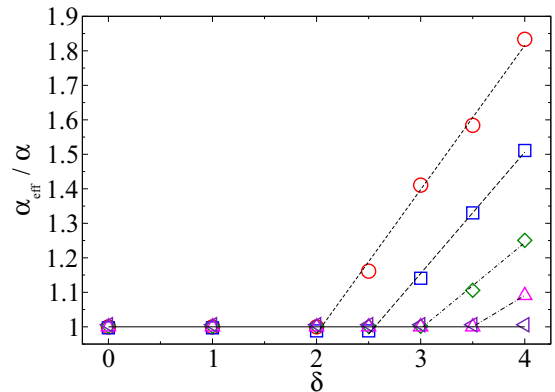


FIG. 4. (Color online) The ratio  $\alpha_{\text{eff}}/\alpha$  as a function of the spatial exponent  $\delta$  for SF networks when the degree exponents are  $\alpha = 2.25$  ( $\circ$ ),  $2.50$  ( $\square$ ),  $2.75$  ( $\diamond$ ),  $3.00$  ( $\triangle$ ),  $3.25$  ( $\triangleleft$ ). The black lines are guidelines. For each parameter set we averaged over 50 configurations.

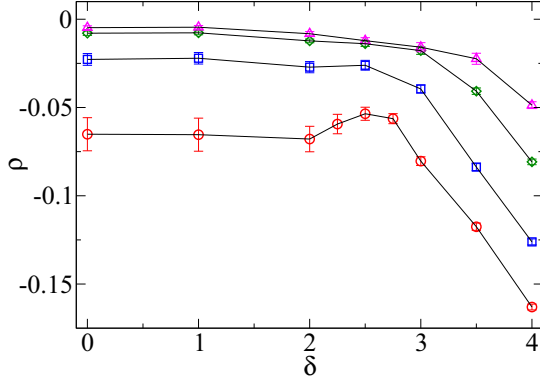


FIG. 5. (Color online) The degree-degree correlation  $\rho$  as a function of the spatial exponent  $\delta$  for SF networks of size  $6.4 \times 10^5$  and degree exponents  $\alpha = 2.25$  ( $\circ$ ),  $2.50$  ( $\square$ ),  $2.75$  ( $\diamond$ ),  $3.00$  ( $\triangle$ ). For each parameter set we averaged over 50 configurations. The error bars refer to the standard deviation.

and  $\alpha$ . By definition truly random networks without spatial constraints [32] have no degree-degree correlations. For spatially embedded networks we expect anticorrelations (disassortativity) to appear since high degree nodes cannot be close to each other due to the spatial constraints. This is particularly true for small  $\alpha$  and large  $\delta$  values.

A quantitative measure for the degree-degree correlations is the degree-degree covariance [33,34],

$$c = \sum_{kl} kl [p(k,l) - p(k)p(l)], \quad (5)$$

where  $p(k,l)$  is the joint probability that two neighboring nodes have degree  $k$  and  $l$  and  $p(l) = \sum_k p(k,l)$  is the probability that any node is linked to a node with  $l$  links. For uncorrelated networks,  $p(k,l) = p(k)p(l)$ . It is easy to see that  $p(k)$  is related to the degree distribution  $P(k)$  by

$$p(k) = \frac{kP(k)}{\sum_l lP(l)}. \quad (6)$$

For the maximum correlation we have  $p(k,l) = p(k)\delta_{k,l}$  and, hence,  $c_{\max} = \sum_k k^2 p(k) - [\sum_k k p(k)]^2$ . It is convenient to normalize  $c$  by dividing by  $c_{\max}$ ,  $\rho = c/c_{\max}$ . Figure 5 shows  $\rho$  for  $\alpha$  in the most relevant regime between 2.25 and 3, for  $\delta$  between 0 and 4. The figure shows that, as expected, negative correlations appear which become stronger when  $\alpha$  decreases and  $\delta$  increases. For each  $\alpha$  value, the anticorrelations are roughly constant for  $\delta < 3$  and increase rapidly for larger  $\delta$ . These anticorrelations are consistent with the changes in  $\alpha^*$  and  $\alpha_{\text{eff}}$ , which both become significantly larger than  $\alpha$ . Note that anticorrelations appear also for  $\delta < 2$ , where spatial constraints are not relevant. These kinds of anticorrelations are due to the fact that the algorithm used for generating SF networks is not fully random (see [33]).

### C. Topological distance

Next we consider the mean topological distance  $\langle \ell \rangle$  in the spatially embedded SF networks. The topological distance between two nodes is the shortest path between them in the network. Without spatial constraints, the networks form an

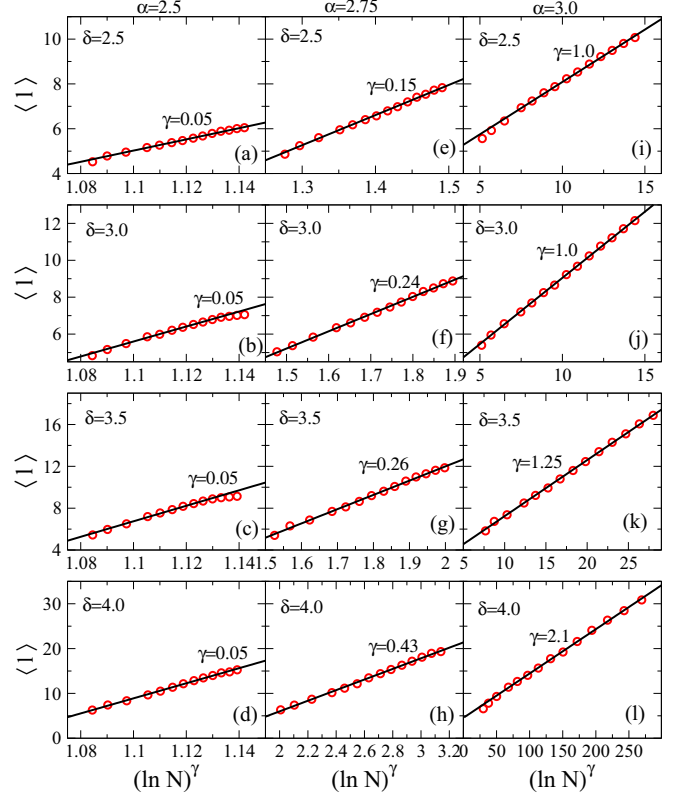


FIG. 6. (Color online) The mean topological distance  $\langle \ell \rangle$  as a function of  $(\ln N)^\gamma$  on SF networks for the spatial exponents  $\delta = 2.5$ ,  $3.0$ ,  $3.5$ , and  $4.0$  (from top to bottom), and for the degree exponents  $\alpha = 2.5$  [panels (a)–(d)],  $\alpha = 2.75$  [panels (e)–(h)], and  $\alpha = 3$  [panels (i)–(l)]. The straight lines are best fits to the data with the slope  $\gamma$ .

ultrasmall world for  $\alpha < 3$  where  $\langle \ell \rangle$  scales with the network size  $N$  as  $\langle \ell \rangle \sim \ln \ln N$  [35], while for  $\alpha > 3$ , the networks only form a small world where  $\langle \ell \rangle$  scales logarithmically with  $N$ ,  $\langle \ell \rangle \sim \ln N$ , as in ER networks [4–6]. At  $\alpha = 3$ ,  $\langle \ell \rangle \sim \ln N / \ln \ln N$  [35]. The question is how might these laws be changed by the spatial constraints? We seek expressions of the form

$$\langle \ell \rangle \sim (\ln N)^\gamma. \quad (7)$$

We assume this form since it can bridge continuously between ultrasmall world behavior ( $\gamma \ll 1$ ), small world behavior ( $\gamma = 1$ ), and large world behavior ( $\gamma \rightarrow \infty$ ), resulting in power laws with  $N$ . For  $\delta$  above 4 we expect a power law dependence on  $N$ . Note that for small exponents  $\gamma$ ,  $(\ln N)^\gamma$  cannot be distinguished from double logarithmic behavior characterizing the ultrasmall world, while for  $\gamma > 1$  we have an intermediate behavior between small world and large world, which has been observed in ER networks with spatial constraints [10].

Figure 6 shows, for  $\alpha = 2.5$ ,  $2.75$ , and  $3$ , the mean topological distance of the spatially embedded networks for  $\delta$  between  $2.5$  and  $4$ , as a function of  $(\ln N)^\gamma$ . The value of the exponent  $\gamma$  has been chosen such that  $\langle \ell \rangle$  increases linearly with  $(\ln N)^\gamma$ . The figure shows that for  $\alpha = 2.5$ , the best fit is  $\gamma$  close to  $0.05$ . Such a small value cannot be distinguished from a  $\ln \ln N$  dependence. This indicates that

the mean topological distance increases with  $N$  significantly slower than logarithmically; i.e., the networks form ultrasmall worlds. The same holds for  $\alpha = 2.75$ , but now the exponents  $\gamma$  are considerably larger, ranging from  $\gamma = 0.15$  for  $\delta = 2.5$  to  $\gamma = 0.43$  for  $\delta = 4$ . These results suggest that for  $\alpha$  below 3, the spatially embedded networks belong to the universality class of ultrasmall worlds in the intermediate regime between  $\delta = 2$  and 4.

For  $\alpha = 3$ ,  $\langle \ell \rangle$  still can be described by a power law of  $\ln N$ , but now the exponent  $\gamma$  is greater than or equal to 1 and increases with  $\delta$ . At  $\delta = 1$  and 2, we expect  $\langle \ell \rangle \sim \ln N / \ln \ln N$ , but for distinguishing this behavior from the simple logarithmic behavior, considerably larger networks are needed. At  $\delta = 4$ ,  $\gamma = 2.1$ . We obtained a similar behavior for  $\alpha = 3.5$ , with exponents  $\gamma$  greater than 1 as long as  $\delta < 4$ , while at  $\delta = 4$ ,  $\langle \ell \rangle$  increases by a power law,  $\langle \ell \rangle \sim N^{1/d_\ell}$ , where  $d_\ell \simeq 4$ . This value is close to the value  $d_\ell \simeq 3.67$  found for ER networks with  $\delta = 4$  [10,13]. Accordingly, regarding the scaling of the mean topological distance  $\langle \ell \rangle$  with the system size, the SF networks with  $\alpha = 3.5$  behave as spatially embedded ER networks [10].

#### D. Dimension of the embedded networks

For studying the dimension of the spatially embedded SF networks we follow the method described in [20]. A similar technique has been used before in disordered systems to calculate the fractal dimension; see, e.g., [36]. We use the fact that the mass  $M$  (number of nodes) of an object within an hypersphere of radius  $r$  scales with  $r$  as

$$M \sim r^d, \quad (8)$$

where the exponent  $d$  represents the dimension of the network. When using this relation without taking into account the way the nodes are linked, one trivially and erroneously finds that the dimension of the network is identical to the dimension  $d_e$  of the embedding space. To properly take into account the connectivity when considering the dimension of the network, we proceed as follows: We choose a node as origin and determine its nearest neighbors (referred to as shell  $\ell = 1$ ) and their number  $S(1)$ , the number of second nearest neighbors  $S(2)$  in shell  $\ell = 2$ , and so on. Next we measure the mean Euclidean distance  $r(\ell)$  of the nodes in shell  $\ell$  from the origin and determine the number of nodes  $M(\ell) = \sum_{i=1}^{\ell} S(i)$  within shell  $\ell$ . To improve the statistics, we repeat the calculations for many origin nodes and then average  $r(\ell)$  and  $M(\ell)$ . To reduce finite size effects, we do not choose the origin nodes randomly in the underlying lattice, but from a region with radius  $L/10$  around the central node. From the scaling relation between the average  $M$  and the average  $r$ , Eq. (8), we determine the dimension  $d$  of the network.

When applying this method to embedded ER-type networks we found [13] that the dimension  $d$  of the network changes with  $\delta$ . For  $\delta$  below the embedding dimension  $d_e$ ,  $d$  is infinity, while for  $\delta$  between  $d_e$  and  $2d_e$  the dimension decreases continuously from infinity to  $d_e$ . Figure 7 shows, in a double logarithmic presentation, for  $\alpha = 2.75$  and 3.5 the mass  $M$  (within a radius  $r$ ) of SF embedded networks as a function of  $r$  for four  $\delta$  values. For  $\alpha = 2.75$  [Fig. 7(a)] the curves bend up continuously, suggesting an infinite dimension. In contrast,

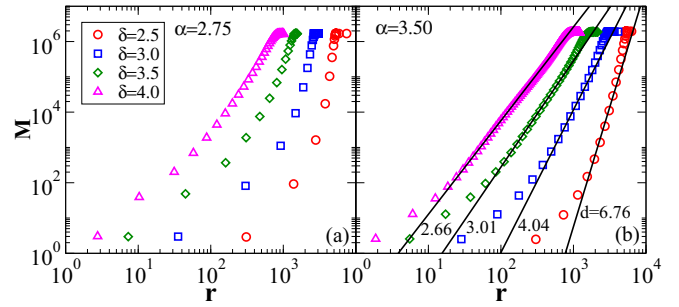


FIG. 7. (Color online) The mass  $M$  as function of the Euclidean distance  $r$  for SF networks embedded in an  $1600 \times 1600$  lattice, for the spatial exponents  $\delta = 2.5, 3.0, 3.5, 4.0$  (from right to left) and the degree exponents  $\alpha = 2.75$  (a) and  $\alpha = 3.50$  (b). The straight lines in panel (b) are guidelines that yield the dimensions of the embedded networks  $d = 2.66, 3.01, 4.04, 6.76$  (from left to right). For transparency the right plots in each panel have been shifted horizontally by factors of 2.

for  $\alpha = 3.5$  [Fig. 7(b)] there seems to be a large regime where  $M$  increases by a power law (constant slope  $d$ ) suggesting finite dimensions: For  $\delta = 2.5, 3, 3.5$ , and 4, the dimensions are  $d = 6.76, 4.04, 3.01$ , and 2.66, respectively.

These findings are consistent with our results for the mean topological distance shown in Fig. 6. For  $\alpha$  below 3,  $\langle \ell \rangle$  increases with the system size  $N$  slower than logarithmically (ultrasmall world), and thus we expect an infinite dimension. In contrast, for  $\alpha$  above 3,  $\langle \ell \rangle$  increases with  $N$  faster than logarithmically, and thus we anticipate a finite dimension. Following this argument, we expect a finite dimension also for  $\alpha = 3$  when  $\delta$  is 3.5 or 4. However, a direct measurement of  $d$  using  $M$  versus  $r$  is difficult due to large finite size effects and much larger systems are needed to test our hypothesis. Note that in our earlier study [20] we suggested (in contrast to the present result) that also for  $\alpha$  below 3 and  $\delta = 3$  the embedded SF network had a finite dimension. The reason for this discrepancy is that in [20] the algorithm for generating the embedded network was suitable for ER networks but not for SF networks.

#### E. Robustness of the networks

The dependence of the mean topological distance on the system size should have important implications on the percolation properties of the spatially embedded networks. For SF networks without spatial constraints we know [31] that for  $\alpha$  between 2 and 3, the percolation threshold  $p_c$  approaches zero with increasing system size  $N$ ,

$$p_c \sim N^{-\lambda}. \quad (9)$$

In uncorrelated networks, it is known that  $p_c \sim k_{\max}^{-(3-\alpha)} \sim N^{-(3-\alpha)/(\alpha-1)}$  and thus  $\lambda = (3-\alpha)/(\alpha-1)$ . In this case,  $p_c$  tends to zero in the thermodynamic limit, and the networks are extremely robust. For  $\alpha$  above 3, like in ER networks,  $p_c$  is finite; i.e., removing randomly a finite fraction of the network nodes is sufficient to destroy the network. The question is how the spatial constraints affect the vulnerability of the SF networks.

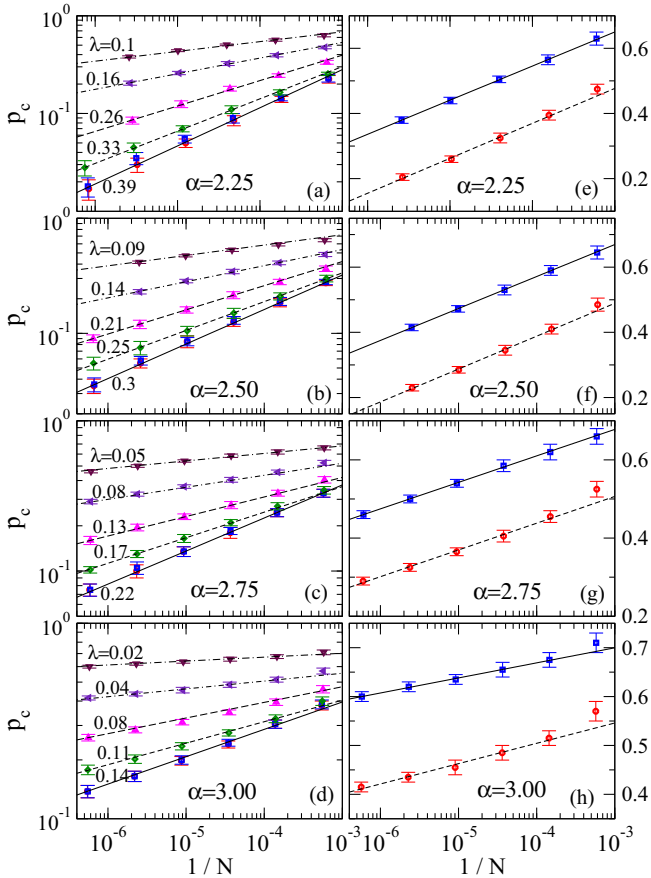


FIG. 8. (Color online) Panels (a)–(d): The critical concentration  $p_c$  as function of  $1/N$  for SF networks (log-log scale). The degree exponents are  $\alpha = 2.25$  (a),  $2.50$  (b),  $2.75$  (c), and  $3.0$  (d), and the length exponents are  $\delta = 1.0$  ( $\circ$ ),  $2.0$  ( $\square$ ),  $2.5$  ( $\diamond$ ),  $3.0$  ( $\triangle$ ),  $3.5$  ( $\triangleleft$ ), and  $4.0$  ( $\nabla$ ). The black lines are best fits to the data with the slope  $\lambda$ . Panels (e)–(h): The same as the panels (a)–(d) when  $\delta = 3.5$  and  $4$ , but on a semilog scale (to check the logarithmic dependencies). The black lines are guidelines.

Figure 8 shows the critical concentration  $p_c$ , obtained from the position of the maximum of the second largest cluster in the networks [36], as a function of  $1/N$  for SF networks with  $\alpha = 2.25$  (a),  $2.50$  (b),  $2.75$  (c), and  $3.0$  (d), for  $\delta$  between 1 and 4. The figure shows that even for  $\delta = 1$ , where spatial constraints are not relevant, the exponent  $\lambda$  is slightly below the expected value. The reason is that the networks we consider here exhibit anticorrelations induced by the process of generation. With increasing  $\delta$ , the exponent  $\lambda$  decreases significantly; i.e., for a fixed network size, the critical concentration increases strongly with  $\delta$ . At  $\delta = 3.5$  and  $4$ ,  $\lambda$  is quite small, such that the power law decay is hard to distinguish from a logarithmic decay. Panels (e)–(h) show a semilogarithmic plot of  $p_c$  versus  $1/N$  for the same  $\alpha$  values considered before, but only for  $\delta = 3.5$  and  $4$ . The figure suggests that in particular for  $\delta = 4$ , a logarithmic decay is likely. For  $\alpha = 3$ , we also cannot exclude the possibility that  $p_c$  approaches a finite nonzero value when the network size  $N$  approaches infinity, for all values of  $\delta$ . This is indicated in Fig. 9, where we have plotted, for  $\alpha = 3$  and  $3.5$ , and  $\delta$  between 1 and 4,  $p_c$  as function of  $1/N$ , on a linear scale. The possibility that, for  $\alpha = 3$  and  $\delta$  above 2,  $p_c$  will approach

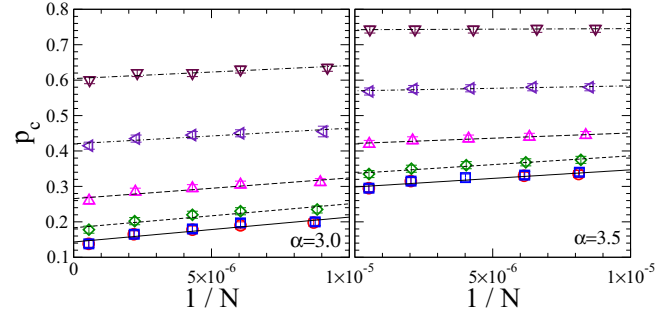


FIG. 9. (Color online) The critical concentration  $p_c$  as function of  $1/N$  on SF networks for the degree exponents  $\alpha = 3.0$  (left panel) and  $3.5$  (right panel). The spatial exponents are  $\delta = 1.0$  ( $\circ$ ),  $2.0$  ( $\square$ ),  $2.5$  ( $\diamond$ ),  $3.0$  ( $\triangle$ ),  $3.5$  ( $\triangleleft$ ), and  $4.0$  ( $\nabla$ ). The black lines are best fits to the data.

a finite value when  $N$  approaches infinity is supported by our findings for the mean topological distance, Fig. 6, where we had shown that for these sets of parameters, the networks are intermediate between small and large world since the mean topological distance increases faster than  $\ln N$ . It is known that for unembedded random SF networks with  $\alpha = 3$ ,  $p_c \sim 1/\ln N$  approaches zero logarithmically [31]. In either case, we expect that for  $\alpha = 3$ ,  $p_c$  decays either logarithmically to zero or approaches a constant with increasing system size, such that we have to assign the value of  $\lambda = 0$  to this case, for all values of  $\delta$ . Figure 10 finally summarizes our findings for the exponent  $\lambda$  that governs the power law decay of  $p_c$  with  $N$ .

### V. CONCLUSION

We developed a method to generate spatially embedded SF networks with a power law distribution of link lengths characterized by the spatial exponent  $\delta$ . The degree of each node was chosen from a power law distribution characterized by the degree exponent  $\alpha$ . In the algorithm, we consider the

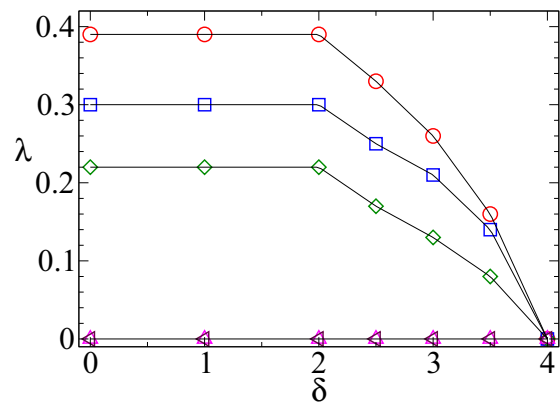


FIG. 10. (Color online) The exponent  $\lambda$  [Eq. (9)] as function of the spatial exponent  $\delta$  on SF networks for the degree exponents  $\alpha = 2.25$ ,  $2.50$ ,  $2.75$ ,  $3$ , and  $3.50$  (from top to bottom). The black lines are guides for the eye. For  $\lambda = 0$ , the critical concentration  $p_c$  either converges, with increasing system size, logarithmically to zero or approaches a finite value.

nodes in a square lattice of size  $L \times L$ , and we link pairs of nodes at distance  $r$  taken from Eq. (1). For fulfilling the constraints coming from both power laws, we had to dilute the network such that only a finite fraction of the  $L^2$  nodes belongs to the network.

When using this method, we find that for  $\delta > 2$  SF networks with degree exponents  $\alpha$  close to and below 2 could not be spatially embedded in two dimensions. For  $\alpha$  between 2.25 and 3, SF networks with  $\delta > 2$  have strong deviations from random nonembedded SF networks. The deviations appear in the dependence of the maximum degree  $k_{\max}$  on the system size  $N$ , in pronounced degree-degree anticorrelations (disassortativity), in significantly larger topological distances, and in a larger vulnerability characterized by larger percolation thresholds.

For example, the topological distance does no longer scale with  $\log N$  or  $\log \log N$  as in nonembedded networks, but usually has the form  $(\log N)^\gamma$  [see Eq. (7)], where  $\gamma$  depends on both  $\alpha$  and  $\delta$ . For  $\alpha$  below 3,  $\gamma$  is below 1 (indicating that the constrained networks have a smaller diameter than

small worlds). For  $\alpha$  greater than or equal to 3,  $\gamma$  is above 1 (indicating that the constrained networks are characterized by a larger diameter than in small worlds). This result suggests that for  $\alpha$  below 3, the dimension  $d$  of the network is infinite, as for the case of unconstrained networks. For  $\alpha$  above 3, the dimension becomes finite and depends on  $\delta$ : For  $\delta$  above 4,  $d$  is equal to the dimension of the embedding lattice, while for  $\delta$  below 4,  $d$  increases with decreasing  $\delta$  and reaches infinity when  $\delta$  approaches 2. For  $\delta$  below 2, the spatial constraints are irrelevant, and the properties are similar to those of random unembedded networks. We believe that these main features should hold qualitatively also for real networks having similar power law distributions.

#### ACKNOWLEDGMENTS

A.B. and S.H. gratefully acknowledge financial support by the Deutsche Forschungsgemeinschaft. S.H. also thanks the MULTIPLEX (EU FET Project No. 317532) and the Israel Science Foundation for financial support.

- 
- [1] R. Albert and A.-L. Barabasi, *Rev. Mod. Phys.* **74**, 47 (2002).
  - [2] A. Barrat, M. Barthélemy, and A. Vespignani, *Dynamical Processes on Complex Networks* (Cambridge University Press, Cambridge, U.K., 2008).
  - [3] R. Cohen and S. Havlin, *Complex Networks: Structure, Robustness, and Function* (Cambridge University Press, Cambridge, U.K., 2010).
  - [4] P. Erdős and A. Rényi, *Publ. Math. Debrecen* **6**, 290 (1959).
  - [5] P. Erdős and A. Rényi, *Publ. Math. Inst. Hung. Acad. Sci.* **5**, 17 (1960).
  - [6] B. Bollobas, *Random Graphs* (Academic Press, London, 1985).
  - [7] R. Albert, H. Jeong, and A.-L. Barabási, *Nature (London)* **401**, 130 (1999).
  - [8] A.-L. Barabási, R. Albert, and H. Jeong, *Physica A* **272**, 173 (1999).
  - [9] A.-L. Barabási, R. Albert, and H. Jeong, *Physica A* **281**, 69 (2000).
  - [10] K. Kosmidis, S. Havlin, and A. Bunde, *Europhys. Lett.* **82**, 48005 (2008).
  - [11] L. Daqing, L. Guanliang, K. Kosmidis, E. H. Stanley, A. Bunde, and S. Havlin, *Europhys. Lett.* **93**, 68004 (2011).
  - [12] T. Emmerich, A. Bunde, and S. Havlin, *Phys. Rev. E* **86**, 046103 (2012).
  - [13] T. Emmerich, A. Bunde, S. Havlin, G. Li, and D. Li, *Phys. Rev. E* **87**, 032802 (2013).
  - [14] C. F. Moukarzel and M. Argollo de Menezes, *Phys. Rev. E* **65**, 056709 (2002).
  - [15] C. F. Moukarzel, *Physica A* **356**, 157 (2005).
  - [16] C. F. Moukarzel, *Physica A* **372**, 340 (2006).
  - [17] G. Bianconi, P. Pin, and M. Marsili, *Proc. Natl. Acad. Sci. U.S.A.* **106**, 11433 (2009).
  - [18] R. Lambiotte, V. D. Blondel, C. de Kerchove, E. Huens, C. Prieur, Z. Smoreda, and P. Van Dooren, *Physica A* **387**, 5317 (2008).
  - [19] J. Goldberg and M. Levy, [arXiv:0906.3202](https://arxiv.org/abs/0906.3202).
  - [20] L. Daqing, K. Kosmidis, A. Bunde, and S. Havlin, *Nat. Phys.* **7**, 481 (2011).
  - [21] D. J. Watts and S. H. Strogatz, *Nature (London)* **393**, 440 (1998).
  - [22] D. J. Watts, *Small Worlds* (Princeton University Press, Princeton, NJ, 1999).
  - [23] J. M. Kleinberg, *Nature (London)* **406**, 845 (2000).
  - [24] A. F. Rozenfeld, R. Cohen, D. ben-Avraham, and S. Havlin, *Phys. Rev. Lett.* **89**, 218701 (2002).
  - [25] S. S. Manna and P. Sen, *Phys. Rev. E* **66**, 066114 (2002).
  - [26] C. P. Warren, L. M. Sander, and I. M. Sokolov, *Phys. Rev. E* **66**, 056105 (2002).
  - [27] R. Xulvi-Brunet and I. M. Sokolov, *Phys. Rev. E* **66**, 026118 (2002).
  - [28] G. Li, S. D. S. Reis, A. A. Moreira, S. Havlin, H. E. Stanley, and J. S. Andrade, Jr., *Phys. Rev. Lett.* **104**, 018701 (2010).
  - [29] G. Li, S. D. S. Reis, A. A. Moreira, S. Havlin, H. E. Stanley, and J. S. Andrade, Jr., *Phys. Rev. E* **87**, 042810 (2013).
  - [30] P. Hines, S. Blumsack, E. Cotilla Sanchez, and C. Barrows, Proceedings of the 43rd Hawaii International Conference on System Sciences (unpublished).
  - [31] R. Cohen, K. Erez, D. ben-Avraham, and S. Havlin, *Phys. Rev. Lett.* **85**, 4626 (2000).
  - [32] M. Molloy and B. Reed, *Random Struct. Algorithms* **6**, 161 (1995).
  - [33] D. S. Callaway, J. E. Hopcroft, J. M. Kleinberg, M. E. J. Newman, and S. H. Strogatz, *Phys. Rev. E* **64**, 041902 (2001).
  - [34] M. E. J. Newman, *Phys. Rev. Lett.* **89**, 208701 (2002).
  - [35] R. Cohen and S. Havlin, *Phys. Rev. Lett.* **90**, 058701 (2003).
  - [36] A. Bunde and S. Havlin, *Fractals and Disordered System* (Springer Verlag, Heidelberg, Berlin, New York, 1996).